The fleet size and mix pollution-routing problem

Çağrı Koç [a], Tolga Bektaş [a,*], Ola Jabali [b], Gilbert Laporte [c]

[a] CORMSIS and Southampton Business School, University of Southampton, Southampton SO17 1BJ, United Kingdom
[b] CIRRELT and HEC Montréal, 3000, chemin de la Côte-Sainte-Catherine, Montréal H3T 2A7, Canada
[c] CIRRELT and Canada Research Chair in Distribution Management, HEC Montréal, 3000, chemin de la Côte-Sainte-Catherine, Montréal H3T 2A7, Canada

Article history:
Received 14 May 2014
Received in revised form 2 September 2014
Accepted 13 September 2014

1. Introduction

Road freight transport is a primary source of greenhouse gases (GHGs) emissions such as carbon dioxide (CO_2), the amount of which is directly proportional to fuel consumption (Kirby et al., 2000). In the United Kingdom and in the United States, around a quarter of GHGs comes from freight transportation (DfT, 2012; EPA, 2012). Greenhouse gases mainly result from burning fossil fuel, and over 90% of the fuel used for freight transportation is petroleum-based, which includes gasoline and diesel. These sources account for over half of the emissions from the transportation sector (Ribeiro et al., 2007).

Demir et al. (2011) have analyzed several models for fuel consumption and greenhouse gas emissions in road freight transportation. Specifically, the authors have compared six models and have assessed their respective strengths and weaknesses. These models indicate that fuel consumption depends on a number of factors that can be grouped into four categories: vehicle, driver, environment and traffic. The pollution-routing problem (PRP), introduced by Bektaş and Laporte (2011), is an extension of the classical vehicle routing problem with time windows (VRPTW). It consists of routing vehicles to serve a set of customers, and of determining their speed on each route segment to minimize a function comprising fuel cost, emissions and driver costs. To estimate pollution, the authors apply a simplified version of the emission and fuel consumption model proposed by Barth et al. (2005), Scora and Barth (2006), Barth and Boriboonsomsin (2009). The simplified model assumes that in a vehicle trip all parameters will remain constant on a given arc, but load and speed may change from one arc to another. As such, the PRP model approximates the total amount of energy consumed on a given road segment, which directly translates into fuel consumption and further into GHG emissions. Demir et al. (2012) have developed an extended adaptive large neighborhood search (ALNS) heuristic for the PRP. This heuristic operates in two stages: the first stage is an extension of the classical ALNS scheme to construct vehicle routes (Pisinger and Ropke, 2007; Ropke and

* Corresponding author. Tel.: +44 2380598969.
E-mail addresses: C.Koc@soton.ac.uk (Ç. Koç), T.Bektas@soton.ac.uk (T. Bektaş), Ola.Jabali@hec.ca (O. Jabali), Gilbert.Laporte@cirrelt.ca (G. Laporte).

Pisinger, 2006a,b) and the second stage applies a speed optimization algorithm (SOA) (Norstad et al., 2010; Hvattum et al., 2013) to compute the speed on each arc. In a later study, Demir et al. (2014a) have introduced the bi-objective PRP which jointly minimizes fuel consumption and driving time. The authors have developed a bi-objective adaptation of their ALNS-SOA heuristic and compared four *a posteriori* methods, namely the weighting method, the weighting method with normalization, the epsilon-constraint method and a new hybrid method, using a scalarization of the two objective functions.

The trade-off between minimizing CO_2 emissions and minimizing total travel times was studied by Jabali et al. (2012) in the context of the time-dependent vehicle routing problem. The planning horizon was partitioned into two phases: free flow traffic and congestion. The authors solved the problem via a tabu search and proposed efficient bounding procedures. Franceschetti et al. (2013) have later introduced the time-dependent pollution-routing problem where a two-stage planning horizon was used, as in Jabali et al. (2012). Such a treatment has allowed for an explicit modeling of congestion in addition to the PRP objectives. The authors developed an integer linear programming formulation in which vehicle speeds are optimally selected from a set of discrete values. Kopfer and Kopfer (2013) studied the emission minimization vehicle routing problem while considering a heterogeneous fleet. These authors described a mathematical formulation for the problem and computed the CO_2 emissions based on the payload and on the traveled distance. They presented results of computational experiments performed on small size instances with up to 10 customers. Kopfer et al. (2014) have analyzed the potential of reducing CO_2 emissions achievable by using an unlimited heterogeneous fleet of vehicles of different sizes. Kwon et al. (2013) have considered the heterogeneous fixed fleet vehicle routing problem with the objective of minimizing carbon emissions. They presented a mathematical model enabling them to perform a cost-benefit assessment of the value of purchasing or selling carbon emission rights. CO_2 emissions are calculated by fuel consumption which is based on the traveled distance of the vehicles. An upper limit for the amount of CO_2 was considered in order to introduce more flexibility into an environmentally constrained network. The authors developed tabu search algorithms and suggested that the amount of carbon emission can be reduced without sacrificing the cost because of the benefit obtained from carbon trading. For other relevant references and a state-of-the-art coverage on green road freight transportation, the reader is referred to the survey of Demir et al. (2014b).

In most real-world distribution problems, customer demands are met with heterogeneous vehicle fleets (Hoff et al., 2010). Two major problems belonging to this category are the fleet size and mix vehicle routing problem introduced by Golden et al. (1984), which works with an unlimited heterogeneous fleet, and the heterogeneous fixed fleet vehicle routing problem proposed by Taillard (1999), which works with a known fleet. These two main problems are reviewed by Baldacci et al. (2008) and Baldacci and Mingozzi (2009). To our knowledge, the fleet size and mix vehicle routing problem combining time windows with the PRP objectives, has not yet been investigated. We believe there is merit in analyzing and solving the fleet size and mix pollution-routing problem (FSMPRP), not only to quantify the benefits of using a flexible fleet with respect to fuel, emissions and the relevant costs, but also to overcome the necessary methodological challenges to solve the problem.

The contributions of this paper are threefold. First, we introduce the FSMPRP as a new PRP variant. The second contribution is to develop a new metaheuristic for the FSMPRP. Our third contribution is to perform analyses in order to provide managerial insights, using the FSMPRP model and several variants. These analyses shed light on the trade-offs between various method components and performance measures, such as distance, fuel and emissions, enroute time and vehicle types. They also highlight and quantify the benefits of using a heterogeneous fleet of vehicles over a homogeneous fleet.

The remainder of this paper is structured as follows. Section 2 presents a background on vehicle types and characteristics. Section 3 provides a formal description of the FSMPRP and the mathematical formulation. Section 4 contains a detailed description of the metaheuristic. Computational experiments and analyses are presented in Section 5, followed by conclusions in Section 6.

2. Background on vehicle types and characteristics

Available studies on emission models (e.g., Demir et al., 2011, 2014b) show the significant impact that the vehicle type has on fuel consumption. In a goods distribution context, using smaller capacity vehicles is likely to increase the total distance travelled and may also increase CO_2 emissions. According to Campbell (1995a,b), if large vehicles are replaced by a larger number of small vehicles, emissions are likely to increase, even though a heavy duty vehicle which has a larger engine consumes more fuel per km than a light duty vehicle. According to Kopfer et al. (2014), replacing a large vehicle by several vehicles of different types may sometimes result in a reduction of CO_2 emissions. Vehicle type effects the engine friction factor, engine speed, engine displacement, aerodynamics drag, frontal surface area and vehicle drive train efficiency; vehicle curb-weight and payload, i.e., capacity, also play an important role in routing decisions.

In the United Kingdom, the Department of Environment, Food and Rural Affairs (DEFRA, 2007) considers that higher-power engines do not necessarily result in fuel savings, and although these types of engines usually have a larger residual value, they may not be financially advantageous. The effects of curb weight and payload on fuel consumption have been studied by some authors (Bektaş and Laporte, 2011; Demir et al., 2011). The payload of the vehicle has an impact on inertia force, rolling resistance and road slope force. Demir et al. (2011) point out that when compared with light and medium duty, heavy duty vehicles consume significantly more fuel, primarily due to their weight. From the perspective of payload reduction, a study by Caterpillar (2006) has shown that a 4.4% improvement in fuel savings can be reached through a 4500 kg reduction in payload and in gross weight with respect to an initial weight of 36 tonnes. The corresponding improvement

is 8.8% for an initial weight of 27 tonnes. DEFRA (2012) states that a 17-tonne heavy duty vehicle emits 18% more CO_2 per km when fully loaded, and 18% less CO_2 per km when empty, relative to emissions at half-load.

The curb weight and payload constitute the Gross Vehicle Weight Rating (GVWR) of a vehicle. The United States Federal Highway Administration FHWA (2011) has categorized vehicles into three main types according to the GVWR: light duty, medium duty, and heavy duty. In practice, the prominent truck companies produce mainly three vehicle types for distribution (MAN, 2014a; Mercedes-Benz, 2014; Renault, 2014; Volvo, 2014). In our study, we consider the three main vehicle types of MAN (2014a), shown in Fig. 1, particularly as the market share of the trucks of MAN (2014a) was around 16.3% in Western Europe in 2013 (Statista, 2013). These three vehicle types, i.e., light duty, medium duty and heavy duty, are called TGL, TGM and TGX by MAN (2014a). TGL and TGM are Single-Unit Trucks and TGX is a Single-Trailer Truck (FHWA, 2011).

A list of and values for the common parameters (Demir et al., 2012, 2014a; Franceschetti et al., 2013) for all vehicle types and specific parameters (MAN, 2014a,b,c) for each vehicle type are given in Tables 1 and 2, respectively. For further details on TGL, TGM and TGX vehicles and their engines the reader is referred to MAN (2014a,b,c).

Daily vehicle fixed costs f^h are determined according to the United Kingdom Department for Transport (DfT, 2010). These costs combine the capital cost and the annual fixed cost, which itself includes depreciation, repairs and maintenance, tires, insurance and vehicle excise duty. In this paper, we assume that each vehicle route can be completed in one day, so that we can transform the capital and annual cost values into daily costs.

We use the comprehensive emissions model of Barth et al. (2005), Scora and Barth (2006), and Barth and Boriboonsomsin (2008) to estimate fuel consumption and emissions for a given time instant. This model has already been successfully applied to the PRP by Bektaş and Laporte (2011), Demir et al. (2012, 2014a) and Franceschetti et al. (2013). In what follows, we adapt the comprehensive emissions model to account for the heterogeneous fleet case. The fuel consumption rate FR^h (liter/s) of a vehicle of type h is given by

$$FR^h = \xi(k^h N^h V^h + P^h/\eta)/\kappa, \tag{1}$$

where the variable P^h is the second-by-second engine power output (in kW) of vehicle type h. It can be calculated as

$$P^h = P^h_{tract}/n_{tf} + P_{acc}, \tag{2}$$

where the engine power demand P_{acc} is associated with the running losses of the engine and the operation of vehicle accessories such as air conditioning and electrical loads. We assume that $P_{acc} = 0$. The total tractive power requirement P^h_{tract} (in kW) for a vehicle of type h is

$$P^h_{tract} = (M^h\tau + M^h g\sin\theta + 0.5C^h_d\rho A v^2 + M^h g C_r\cos\theta)v/1000, \tag{3}$$

where M^h is the total vehicle weight (in kg) and v is the vehicle speed (m/s). The fuel consumption F^h (in liters) of vehicle type h over a distance d, is calculated as

$$F^h = k^h N^h V^h \lambda d/v + P^h \lambda\gamma^h d/v, \tag{4}$$

where $\lambda = \xi/\kappa\psi$, $\gamma^h = 1/1000n_{tf}\eta$ and $\alpha = \tau + g\sin\theta + gC_r\cos\theta$ are constants. Let $\beta^h = 0.5C^h_d\rho A^h$ be a vehicle-specific constant. Therefore, F^h can be rewritten as

$$F^h = \lambda(k^h N^h V^h d/v + M^h\gamma^h\alpha d + \beta^h\gamma^h d v^2). \tag{5}$$

In this expression the first term $k^h N^h V^h d/v$ is called the engine module, which is linear in the travel time. The second term $M^h\gamma^h\alpha_{ij}d$ is referred to as the weight module, and the third term $\beta^h\gamma^h d v^2$ is the speed module, which is quadratic in speed. These functions will be used in the objective function of our model.

(a) Light duty vehicle: TGL **(b)** Medium duty vehicle: TGM **(c)** Heavy duty vehicle: TGX

Fig. 1. Three vehicle types (MAN, 2014a).

Table 1
Vehicle common parameters.

Notation	Description	Typical values
ξ	Fuel-to-air mass ratio	1
g	Gravitational constant (m/s^2)	9.81
ρ	Air density (kg/m^3)	1.2041
C_r	Coefficient of rolling resistance	0.01
η	Efficiency parameter for diesel engines	0.45
f_c	Fuel and CO_2 emissions cost (£/liter)	1.4
f_d	Driver wage (£/s)	0.0022
κ	Heating value of a typical diesel fuel (kj/g)	44
ψ	Conversion factor (g/s to L/s)	737
n_{tf}	Vehicle drive train efficiency	0.45
v^l	Lower speed limit (m/s)	5.5 (or 20 km/h)
v^u	Upper speed limit (m/s)	27.8 (or 100 km/h)
θ	Road angle	0
τ	Acceleration (m/s^2)	0

Table 2
Vehicle specific parameters.

Notation	Description	Light duty (L)	Medium duty (M)	Heavy duty (H)
w^h	Curb weight (kg)	3500	5500	14,000
Q^h	Maximum payload (kg)	4000	12,500	26,000
f^h	Vehicle fixed cost (£/day)	42	60	95
k^h	Engine friction factor (kj/rev/liter)	0.25	0.20	0.15
N^h	Engine speed (rev/s)	38.34	36.67	30.0
V^h	Engine displacement (liter)	4.5	6.9	10.5
C_d^h	Coefficient of aerodynamics drag	0.6	0.7	0.9
A^h	Frontal surface area (m^2)	7.0	8.0	10.0

3. Mathematical model for the fleet size and mix pollution-routing problem

The FSMPRP is defined on a complete directed graph $\mathcal{G} = (\mathcal{N}, \mathcal{A})$ where $\mathcal{N} = \{0, \ldots, n\}$ is the set of nodes, $\mathcal{A} = \{(i,j) : i,j \in \mathcal{N}, i \neq j\}$ is the set of arcs, and node 0 corresponds to the depot. The distance from i to j is denoted by d_{ij}. The customer set is $\mathcal{N}_0 = \mathcal{N} \setminus \{0\}$, and each customer i has a positive demand q_i. The index set of vehicle types is denoted by $\mathcal{H}$. If a vehicle arrives at customer i before a_i, it waits until a_i before servicing the node. Furthermore, t_i corresponds to the service time of node $i \in N_0$, which must start within time window $[a_i, b_i]$.

The objective of the FSMPRP is to minimize a total cost function encompassing vehicle, driver, fuel and emissions costs. A feasible solution contains a set of routes for a heterogeneous fleet of vehicles that meet the demands of all customers within their respective predefined time windows. Each customer is visited once by a single vehicle, each vehicle must depart from and return to the depot, to serve a quantity of demand that does not exceed its capacity. Furthermore, the speed of each vehicle on each arc must be determined.

The binary variable x_{ij}^h is equal to 1 if and only if a vehicle of type $h \in \mathcal{H}$ travels on arc $(i,j) \in \mathcal{A}$. The formulation works with a discretized speed function, proposed by Bektaş and Laporte (2011), defined by R non-decreasing speed levels $\bar{v}^r$ $(r = 1, \ldots, R)$. The binary variable z_{ij}^{rh} is equal to 1 if and only if a vehicle of type $h \in \mathcal{H}$ travels on arc $(i,j) \in A$ at speed level $r = 1, \ldots, R$, y_j is the service start time at $j \in \mathcal{N}_0$. The total time spent on a route in which $j \in \mathcal{N}_0$ is the last visited node before returning to the depot is defined by s_j. Furthermore, let f_{ij}^h be the amount of commodity flowing on arc $(i,j) \in \mathcal{A}$ by a vehicle of type h. Therefore, the total load of vehicle of type h on arc (i,j) is $w^h + f_{ij}^h$. We now present an integer linear programming formulation for the FSMPRP:

$$\text{(FSMPRP) Minimize} \sum_{h\in\mathcal{H}} \sum_{(i,j)\in\mathcal{A}} \lambda f_c k^h N^h V^h d_{ij} \sum_{r=1}^{R} z_{ij}^{rh} / \bar{v}^r \tag{6}$$

$$+ \sum_{h\in\mathcal{H}} \sum_{(i,j)\in\mathcal{A}} \lambda f_c \gamma^h \alpha_{ij} d_{ij} (w^h x_{ij}^h + f_{ij}^h) \tag{7}$$

$$+ \sum_{h\in\mathcal{H}} \sum_{(i,j)\in\mathcal{A}} \lambda f_c \beta^h \gamma^h d_{ij} \sum_{r=1}^{R} (\bar{v}^r)^2 z_{ij}^{rh} \tag{8}$$

$$+ \sum_{j\in\mathcal{N}_0} f_d s_j + \sum_{h\in\mathcal{H}} \sum_{j\in\mathcal{N}_0} f_h x_{0j}^h \tag{9}$$

subject to

$$\sum_{j\in\mathcal{N}_0} x_{0j}^h \leqslant m_h \quad \forall h \in \mathcal{H} \tag{10}$$

$$\sum_{h\in\mathcal{H}}\sum_{j\in\mathcal{N}} x_{ij}^h = 1 \quad \forall i \in \mathcal{N}_0 \tag{11}$$

$$\sum_{h\in\mathcal{H}}\sum_{i\in\mathcal{N}} x_{ij}^h = 1 \quad \forall j \in \mathcal{N}_0 \tag{12}$$

$$\sum_{h\in\mathcal{H}}\sum_{j\in\mathcal{N}} f_{ji}^h - \sum_{h\in\mathcal{H}}\sum_{j\in\mathcal{N}} f_{ij}^h = q_i \quad \forall i \in \mathcal{N}_0 \tag{13}$$

$$q_j x_{ij}^h \leqslant f_{ij}^h \leqslant (Q^h - q_i) x_{ij}^h \quad \forall (i,j) \in \mathcal{A},\ \forall h \in \mathcal{H} \tag{14}$$

$$y_i - y_j + t_i + \sum_{r=1}^{R} d_{ij} z_{ij}^{rh} / \bar{v}^r \leqslant M_{ij}(1 - x_{ij}^h) \quad \forall i \in \mathcal{N}, j \in \mathcal{N}_0, i \neq j, \forall h \in \mathcal{H} \tag{15}$$

$$a_i \leqslant y_i \leqslant b_i \quad \forall i \in \mathcal{N}_0 \tag{16}$$

$$y_j + t_j - s_j + \sum_{r=1}^{R} d_{j0} z_{j0}^{rh} / \bar{v}^r \leqslant L_{ij}(1 - x_{j0}^h) \quad \forall j \in \mathcal{N}_0 \tag{17}$$

$$\sum_{r=1}^{R} z_{ij}^{rh} = x_{ij}^h \quad \forall (i,j) \in \mathcal{A}, \forall h \in \mathcal{H} \tag{18}$$

$$x_{ij}^h \in \{0,1\} \quad \forall (i,j) \in \mathcal{A}, \forall h \in \mathcal{H} \tag{19}$$

$$z_{ij}^{rh} \in \{0,1\} \quad \forall (i,j) \in \mathcal{A}, r = 1,\ldots,R, \forall h \in \mathcal{H} \tag{20}$$

$$f_{ij}^h \geqslant 0 \quad \forall (i,j) \in \mathcal{A}, \forall h \in \mathcal{H} \tag{21}$$

$$y_i \geqslant 0 \quad \forall i \in \mathcal{N}_0. \tag{22}$$

The first three terms of the objective function represent the cost of fuel consumption and of CO_2 emissions. In particular, term (6) computes the cost induced by the engine module, term (7) reflects the cost induced by the weight module and term (8) measures the cost induced by the speed module. Finally, term (9) computes the total driver wage and the sum of all vehicle fixed costs.

The maximum number of vehicles available for each type is imposed by constraints (10). We consider an unlimited number of vehicles for each vehicle type h ($m_h = |\mathcal{N}_0|$). Constraints (11) and (12) ensure that each customer is visited exactly once. Constraints (13) and (14) define the flows. Constraints (15)–(17) are time window constraints, where $M_{ij} = \max\{0, b_i + s_i + d_{ij}/\bar{v}^r - a_j\}$ and $L_{ij} = \max\{0, b_j + t_j + \max_i\{d_{ij}\}/\bar{v}^r\}$. Constraints (18) impose that only one speed level is selected for each arc. Finally, constraints (19)–(22) enforce the integrality and nonnegativity restrictions on the variables.

4. Description of the hybrid evolutionary algorithm

This section describes the proposed hybrid evolutionary algorithm, called HEA++, for the FSMPRP. This algorithm builds on the HEA of Koç et al. (2014), which is itself based on the principles put forward by Vidal et al. (2014). In this paper, we have additionally developed the Heterogeneous Adaptive Large Neighborhood Search (HALNS) which is used as a main Higher education component in the HEA++. An adapted version of the Speed Optimization Algorithm (SOA) (Norstad et al., 2010; Hvattum et al., 2013) is applied on a solution within the algorithm to optimize speeds between nodes. The combination of ALNS and SOA has provided good results for the PRP (Demir et al., 2012, 2014a).

The general framework of the HEA++ is sketched in Algorithm 1. We now explain the steps of the algorithm in reference to each line of Algorithm 1. The initial population is generated by using a modified version of the classical Clarke and Wright (1964) savings algorithm and the HALNS (line 1). A binary tournament process selects two parents from the population (line 3) and combines them into a new offspring C via crossover (line 4), which then undergoes an improvement step through an advanced Split algorithm with Speed Optimization Algorithm (Ssoa)(line 5). The Ssoa considers offspring C as an input, in the form of a giant tour and then optimally splits it into vehicle routes. In the Higher education procedure, the HALNS with the SOA (line 6) are applied to offspring C. If C is infeasible, this procedure is iteratively applied until a modified version of C is feasible, which is then inserted into the population. The probabilities associated with the Higher education procedure operators are updated by the adaptive weight adjustment procedure (AWAP) (line 7). The Intensification procedure is based on the HALNS and SOA (line 8), and is run on elite solutions. The population size n_a is limited by $n_p + n_o$, where n_p is a constant denoting the size of the initial population and n_o is a constant showing the maximum allowable number of offsprings that can be inserted into the population. A survivor selection mechanism is applied (line 9) if the populations size n_a reaches $n_p + n_o$ at any iteration. Mutation (line 10) is applied to a randomly selected individual from the population with probability p_m at each iteration of the algorithm. The entire population undergoes a Regeneration (line 11) procedure if there are no improvements in the best known solution for a given number of consecutive iterations υ. When the number ϖ of iterations without improvement in the incumbent solution is reached, the HEA++ terminates (line 13). For further implementation details on

the initialization, parent selection, crossover, AWAP, survivor selection and diversification sections the reader is referred to Koç et al. (2014).

In what follows we detail the algorithmic features specifically developed for the FSMPRP. The expanded version of the SOA is presented in Section 4.1, Ssoa is described in Section 4.2, and finally, the Higher education and Intensification procedures are detailed in Section 4.3.

Algorithm 1. General framework of the HEA

1: *Initialization*: initialize a population with size n_p
2: **while** number of iterations without improvement $< \varpi$ **do**
3: *Parent selection*: select parent solutions P_1 and P_2
4: *Crossover*: generate offspring C from P_1 and P_2
5: Ssoa: partition C into routes
6: Higher Education: educate C with HALNS and SOA and insert into population
7: AWAP: update probabilities of the HALNS operators
8: Intensification: intensify elite solution with HALNS and SOA
9: *Survivor selection*: if the population size n_a reaches $n_p + n_o$, then select survivors
10: Mutation: diversify a random solution with probability p_m
11: If number of iterations without improvement $= \upsilon$ **then**
12: Regeneration: diversify the population with Regeneration procedures
13: **end while**
14: Return best feasible solution

4.1. Speed optimization algorithm

The SOA optimizes the speed on each segment of a given route in order to minimize an objective function comprising fuel consumption costs and driver wages. Demir et al. (2012) adapted the arguments of Norstad et al. (2010) and Hvattum et al. (2013) to the PRP, which we describe here for the sake of completeness.

The SOA is defined on a feasible path $(0, \ldots, n+1)$ of nodes all served by a single vehicle, where 0 and $n+1$ are two copies of the depot. The speed v_{i-1}, represents the variable speed between nodes $i-1$ and i, $\underline{e}_i$ is the arrival time at node i and $\overline{e}_i$ is the departure time from node i. The detailed pseudo-code of the SOA is shown in Algorithm 2. The SOA starts with a feasible route with initial fixed speeds, it takes input parameters start node s and end node e, D and T which are respectively the total distance and total service time, and returns speed-optimized routes. Initially, the speed v_{i-1}, for each link is calculated by considering the total distance of the route and the total trip duration without the total service time (lines 4–7 of Algorithm 2). The SOA runs in two stages where the main difference between these stages is the optimal speed v^*_{i-1} calculation (line 8 of Algorithm 2). In the first stage, optimal speeds are calculated as

$$v^* = \left(\frac{k^h N^h V^h}{2\beta^h \gamma^h} + \frac{f_d}{2\beta^h \lambda \gamma^h f_c} \right)^{1/3}, \tag{23}$$

which minimizes fuel consumption and driver wage. The first stage fixes the arrival time to the depot and uses this value as an input to the second stage where optimal speeds are calculated using

$$v^* = \left(\frac{k^h N^h V^h}{2\beta^h \gamma^h} \right)^{1/3}, \tag{24}$$

which minimizes fuel consumption in the second stage. The speeds are updated (lines 9–12 of Algorithm 2) if the vehicle arrives before a_i and departs before b_i or if the vehicle arrives before b_i and departs after $b_i + t_i$. If node i is the last customer before the depot, the speeds are recalculated to arrive at node i at a_i (lines 13–14 of Algorithm 2). If v_{i-1} is lower than v^l, then it is increased to v^l, or if it is greater than v^u, then it is decreased to v^u (lines 15–18 of Algorithm 2). The optimal speed is then compared with v_{i-1}, if the optimal speed is greater, v_{i-1} is then increased to the optimal speed (lines 19–20 of Algorithm 2). The new arrival and departure times at node i are then calculated (lines 21–23 of Algorithm 2). If the departure time is less than $a_i + t_i$ or if the arrival time is greater than b_i, the violation is calculated; otherwise, it is set to zero (lines 24–27 of Algorithm 2). At each iteration, the SOA selects the arc with largest time window violation and eliminates the violation.

4.2. The Split algorithm with the speed optimization algorithm

The Split algorithm for heterogeneous vehicle routing problems (Prins, 2009), takes a giant tour as an input and optimally splits it into vehicle routes. The splitting procedure is based on solving the corresponding shortest path problem. Many extensions of the Split algorithm have been successfully applied in evolutionary based heuristics for several routing problems

(Prins, 2009; Koç et al., 2014; Vidal et al., 2014). Koç et al. (2014) have developed an advanced Split algorithm for a heterogeneous fleet. This algorithm was embedded in the HEA to segment a giant tour and to determine the optimal fleet mix through a controlled exploration of infeasible solutions (Cordeau et al., 2001; Nagata et al., 2010). Time windows and capacity violations are penalized through a term in the objective function. Here we introduce a new algorithmic feature, the Split algorithm with the speed optimization algorithm (Ssoa) in which we incorporate the SOA within the procedure for computing the cost of each arc in the shortest path problem.

Algorithm 2. Speed Optimization Algorithm (s, e)

Input: $violation \leftarrow 0, p \leftarrow 0, D \quad \sum_{i=s}^{e-1} d_i, T \leftarrow \sum_{i=s}^{e} t_i$
Output: Speed optimized routes
for $i = s+1$ **to** e **do**
  if $\underline{e}_s \leqslant a_s$ **then**
    $v_{i-1} \leftarrow D/(\overline{e}_e - a_s - T)$
  else
    $v_{i-1} \leftarrow D/(\overline{e}_e - \underline{e}_s - T)$
  $v^*_{i-1} \leftarrow$ Optimal speed by Eqs. (23) or (24)
  if $\overline{e}_{i-1} + d_{i-1}/v_{i-1} < a_i$ *and* $\overline{e}_i \geqslant a_i + t_i$ *and* $i \neq n$ **then**
    $v_{i-1} \quad d_{i-1}/(a_i - \overline{e}_{i-1})$
  else if $\overline{e}_{i-1} + d_{i-1}/v_{i-1} < b_i$ *and* $\overline{e}_i \geqslant b_i + t_i$ *and* $i \neq n$ **then**
    $v_{i-1} \quad d_{i-1}/(b_i - \overline{e}_{i-1})$
  if $i = n$ *and* $\overline{e}_i \neq \underline{e}_i$ **then**
    $v_{i-1} \quad d_{i-1}/(a_i - \overline{e}_{i-1})$
  if $v_{i-1} < v^l$ **then**
    $v_{i-1} \quad v^l$
  else if $v_{i-1} > v^u$ **then**
    $v_{i-1} \quad v^u$
  if $v^*_{i-1} > v_{i-1}$ **then**
    $v_{i-1} \quad v^*_{i-1}$
  $\underline{e}_i \leftarrow \overline{e}_{i-1} + d_{i-1}/v_{i-1}$
  if $i \neq n+1$ **then**
    $\overline{e}_i = \underline{e}_i + t_i$
  $g_i \leftarrow \max\{0, \underline{e}_i - b_i, a_i + t_i - \overline{e}_i\}$
  if $g_i > violation$ **then**
    $violation \leftarrow g_i$
    $p \leftarrow i$
end for
if $violation > 0$ and $\underline{e}_p > b_p$ **then**
  $\overline{e}_p \leftarrow b_p + t_p$
  Speed Optimization Algorithm (s, p)
  Speed Optimization Algorithm (p, e)
if $violation > 0$ and $\overline{e}_p < a_p + t_p$ **then**
  $\overline{e}_p \leftarrow a_p + t_p$
  Speed Optimization Algorithm (s, p)
  Speed Optimization Algorithm (p, e)

4.3. Higher Education and Intensification

The classical ALNS scheme is based on the idea of gradually improving a starting solution by using both destroy and repair operators on a given fleet mix composition. The ALNS in Koç et al. (2014) uses nine removal and three insertion operators, selected from those employed by various authors (Ropke and Pisinger, 2006a,b; Pisinger and Ropke, 2007; Paraskevopoulos et al., 2008; Demir et al., 2012).

The ALNS is essentially a node improvement procedure and therefore does not explicitly account for the heterogenous fleet dimension. In this paper, we propose the HALNS which integrates fleet sizing within the removal and the insertion operators. For the destroy phase of the HALNS, if a node is removed, we check whether the total demand of the resulting route whether can be served by a smaller vehicle and we update the solution accordingly. For the repair phase of the HALNS, if inserting a node requires additional vehicle capacity, i.e., if the current vehicle cannot satisfy the total customer demand, then we consider the option of using larger vehicle.

We redefine seven removal operators for the destroy phase of the HALNS procedure: worst distance, worst time, neighborhood, Shaw, proximity-based, time-based and demand-based. Furthermore, we redefine three insertion operators for the

repair phase: greedy insertion, greedy insertion with noise function and greedy insertion with en-route time. Each operator has its own specific cost calculation mechanism. Aside from the distance calculations, we account for the difference in the fixed vehicle cost within each operator.

The removal operators iteratively remove nodes, add them to the removal list L_r, and update the fleet mix composition. The latter operation checks whether a vehicle with a smaller capacity can serve the route after the node removal. The insertion operators iteratively find the least-cost insertion position for node in L_r, where the cost computation includes the potential use of larger vehicles due to increasing the total demand of the route. Therefore, the insertion operators insert the nodes in their best position while updating the fleet mix composition.

For each node $i \in \mathcal{N}_0 \setminus L_r$, let f^h be the current vehicle fixed cost associated with the vehicle serving i. Let $\Delta(i)$ be the saving obtained as a result of using a removal operator on node i, as defined in the ALNS. Let f_r^{h*} be the vehicle fixed cost after removal of node i, i.e., f_r^{h*} is modified only if the route containing node i can be served by a smaller vehicle when removing node i. The saving in vehicle fixed cost can be expressed as $f^h - f_r^{h*}$. Thus, the total savings of removing node $i \in \mathcal{N}_0 \setminus L_r$, denoted $RC(i)$, is calculated as follows for each removal operator:

$$RC(i) = \Delta(i) + (f^h - f_r^{h*}). \tag{25}$$

Given a node $i \in \mathcal{N}_0 \setminus L_r$ in the destroyed solution, we define the insertion cost of node $j \in L_r$ after node i as $\Omega(i,j)$. Let f_a^{h*} be the vehicle fixed cost after the insertion of node i, i.e., f_a^{h*} is modified only if the route containing node i necessitates the use of a larger capacity vehicle after inserting node i. The cost difference in vehicle fixed cost can be expressed as $f_a^{h*} - f^h$. Thus, the total insertion cost of node $i \in \mathcal{N}_0 \setminus L_r$ is $IC(i)$, for each insertion operator is

$$IC(i) = \Omega(i,j) + (f_a^{h*} - f^h). \tag{26}$$

Fig. 2 provides an example of the removal and insertion phases of the HALNS procedure.

Koç et al. (2014) developed a two-phase Intensification procedure whose main idea is to improve the quality of elite individuals through intensifying the search within promising regions of the solutions space. Here we introduce an extended version of this procedure. We apply the HALNS by applying well-performing operators on the elite solutions. Furthermore, we apply the SOA on the intensified elite solutions.

5. Computational experiments and analyses

We now summarize the computational experiments performed in order to assess the performance of the HEA++. This algorithm was implemented in C++ and run on a computer with one gigabyte of RAM and an Intel Xeon 2.6 GHz processor.

We have used the PRP library of Demir et al. (2012) as the test bed. These instances were derived from real geographical distances of United Kingdom cities and are available at http://www.apollo.management.soton.ac.uk/prplib.htm. From this library, we have selected the four largest sets containing 75, 100, 150 and 200 nodes. Each set includes 20 instances, resulting in a total of 80 instances. These PRP instances are coupled with the parameters listed in Tables 1 and 2 for the FSMPRP. All algorithmic parametric values were set as in Koç et al. (2014), where an extensive meta-calibration procedure was applied to generate effective parameter values for the standard heterogeneous fleet vehicle routing problem with time windows.

The aim of the computational experiments is fourfold: (i) to analyse the effect of the metaheuristic components (Section 5.1), (ii) to test the efficiency of the algorithm for the solution of the PRP and the FSMPRP (Section 5.2), (iii) to empirically

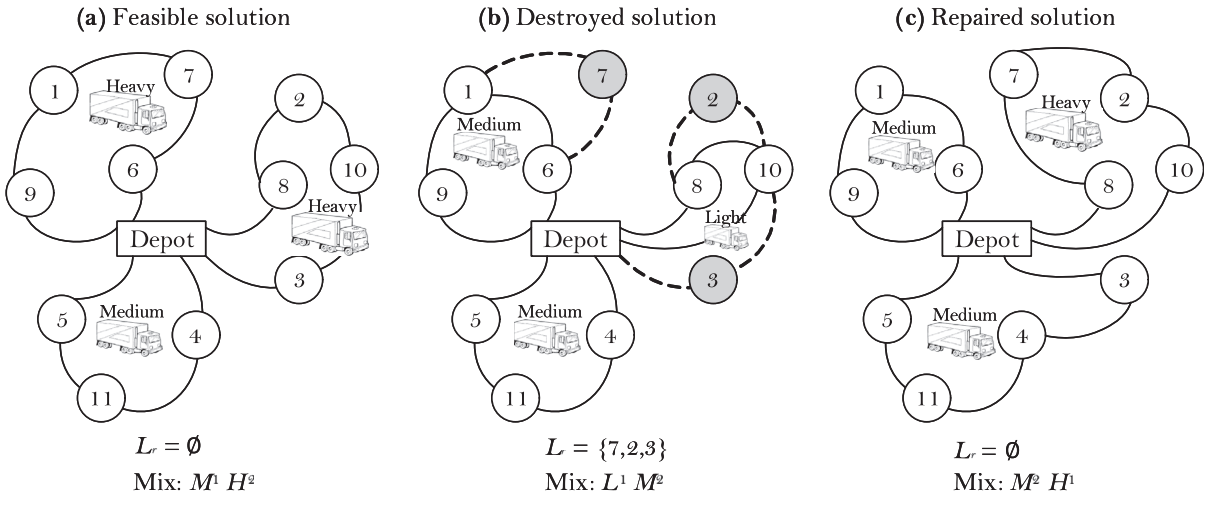

Fig. 2. Illustration of the HALNS procedure.

calculate the savings that could be achieved by using a comprehensive objective function instead of separate objective functions (Section 5.3 (iv) to quantify the benefits of using a heterogeneous fleet over a homogeneous one (Section 5.4).

5.1. Sensitivity analysis on method components

This section compares four versions of the HEA++ the details of which can be found in Table 3. A "No" for HALNS implies using the ALNS of Koç et al. (2014). Similarly, a "No" for SSOA corresponds to using the SPLIT algorithm without SOA. Using the four versions, we present four sets of experiments on the 100-node instances.

Table 4 presents the best results of ten runs on the instances for each of the four versions. The first column displays the instances. The other columns show for each version of the algorithm, the total cost (TC) in £, percentage deterioration in solution quality (Dev) with respect to the HEA++, and the total computational time in minutes (Time). The rows named Avg, Min (%) and Max (%) show the average results, as well as minimum and maximum percentage deviations across all benchmark instances, respectively.

The results clearly indicate the benefits of including the SSOA and HALNS within the HEA++. The HEA++ algorithm is consistently superior to all other three versions on all 20 instances. Version (1) which uses the classical ALNS and SPLIT corresponds to the HEA of Koç et al. (2014), performs worse than all other three versions. The superiority of version (3) over version (2) confirms the importance of the HALNS component in the algorithm. The computation times for all versions are of similar magnitude.

5.2. Results on the PRP and on the FSMPRP

To assess the quality of the HEA++, we have compared our algorithm with that of Demir et al. (2012), referred to as DBL12, by using a homogenous fleet of vehicles with the corresponding vehicle parameters used in the PRP. In Tables 5 and 6, we present the computational results on the PRP instances with 100 and 200 nodes, respectively. The columns show the number of vehicles used in the solution (NV) and the total distance (TD). Ten separate runs were performed for each instance as done by DBL12, the best of which is reported. For each instance, a boldface entry with a "$*$" indicates a new best-known solution.

The results clearly show that HEA++ outperforms DBL12 on all PRP instances in terms of solution quality. The average cost reduction is 1.60% for 100-node instances, for which the minimum and maximum improvements are 0.32% and 2.33%, respectively. For 200-node instances, the corresponding values are 1.72% (average), 0.04% (minimum) and 3.88% (maximum). On average, the Demir et al. (2012) is faster on the 100-node instances, however, this difference is less substantial on the 200-node instances.

Table 7 presents the average results obtained by HEA++ on the 75, 100, 150 and 200-node FSMPRP instances. For each instance set, the columns display the average fuel and CO_2 emissions cost (FEC), driver cost (DC) and vehicle cost (VC). To evaluate the environmental impact of the solutions, we also report the average amount of CO_2 emissions (in kg) based on the assumption that one liter of gasoline contains 2.32 kg of CO_2 (Coe, 2005). For detailed results, the reader is referred to Tables A.1, A.2, A.3, A.4 in the appendix, where ten runs were performed for each instance and the best one is reported. We observe that on average, over all benchmark instances, the vehicle fixed cost accounts for 38.8% of the total cost, whereas the driver cost represents 36.7% of the total, and the fuel and emissions cost accounts for 24.5%.

5.3. The effect of cost components

This section analyzes the implications of using different cost components on the performance measures. To this end, we have conducted experiments using four different objective functions, which are presented in the rows of Table 8. The experiments were conducted on a 100-node FSMPRP instance, and the best results collected over ten runs are reported for each of four performance measures which we will now define. In min TD, we consider the objective of minimizing the total distance. In min FEC, we only consider fuel and emissions cost. This setting also implies minimizing CO_2 since this is proportional to fuel consumption. In min DC, we account only for the driver cost. The min TD + VC objective corresponds to the standard heterogeneous vehicle routing problems, which consists of minimizing distance and vehicle fixed costs. Finally we present the FSMPRP objective. Aside from the objective function values, we provide the main cost components in Table 8. In Table 9, we report the deviations from the smallest cost components shown in Table 8. For example, the minimum value for the total distance objective (min TD) is 1921.66 km, but the FEC objective yields a solution with a total distance of 2119.87 km,

Table 3
Sensitivity analysis experiment setup.

Version	HALNS	SSOA
(1)	No	No
(2)	No	Yes
(3)	Yes	No
HEA++	Yes	Yes

Table 4
Sensitivity analysis of the HEA++ components.

Instance	Version (1)			Version (2)			Version (3)			HEA++	
	TC	Dev	Time	TC	Dev	Time	TC	Dev	Time	TC	Time
UK100_01	1041.82	1.41	5.96	1036.13	0.87	5.28	1035.10	0.77	5.47	1027.10	5.47
UK100_02	1013.75	1.07	4.41	1012.71	0.97	4.27	1007.86	0.50	4.21	1002.87	4.38
UK100_03	948.48	2.99	4.02	942.04	2.33	4.21	925.67	0.60	4.91	920.11	4.65
UK100_04	1001.54	0.92	4.16	1002.47	1.01	4.35	994.98	0.27	4.49	992.32	4.74
UK100_05	955.12	2.47	3.47	944.74	1.40	3.64	939.83	0.88	3.95	931.56	4.21
UK100_06	1053.98	1.49	4.63	1046.18	0.76	4.55	1041.51	0.31	5.19	1038.25	5.63
UK100_07	923.60	1.10	5.39	921.22	0.85	5.41	915.88	0.27	5.47	913.39	5.19
UK100_08	982.33	3.85	3.78	967.55	2.38	4.09	953.08	0.90	4.11	944.51	4.52
UK100_09	933.29	4.53	4.59	909.09	1.99	4.19	898.45	0.83	4.49	891.02	4.69
UK100_10	1008.24	1.87	3.87	992.98	0.36	2.73	991.59	0.22	3.29	989.38	4.19
UK100_11	1054.71	1.87	4.87	1047.71	1.21	3.91	1046.18	1.07	4.19	1034.98	5.13
UK100_12	910.79	3.38	4.26	906.53	2.93	4.27	906.95	2.98	4.52	879.96	4.62
UK100_13	1023.71	2.23	4.46	1021.32	2.00	4.53	1014.79	1.37	4.79	1000.86	4.78
UK100_14	1069.87	1.63	4.69	1063.78	1.06	4.61	1058.20	0.54	4.83	1052.47	5.02
UK100_15	1106.50	2.04	4.57	1091.11	0.66	4.59	1087.32	0.31	4.81	1083.95	5.27
UK100_16	933.25	0.95	4.35	928.36	0.42	4.34	929.98	0.60	4.55	924.42	4.73
UK100_17	1076.11	1.75	3.79	1072.18	1.38	4.29	1066.71	0.88	4.29	1057.33	4.36
UK100_18	956.43	3.52	4.56	935.66	1.37	4.19	924.92	0.23	4.49	922.81	5.01
UK100_19	941.58	1.80	3.67	939.75	1.61	3.81	930.60	0.64	4.99	924.60	4.99
UK100_20	1093.54	3.27	3.43	1070.82	1.22	3.84	1066.49	0.82	4.27	1057.78	4.18
Avg	1001.43	2.21	4.38	992.62	1.34	4.26	986.81	0.75	4.57	979.48	4.79
Min (%)		0.92			0.36			0.22			
Max (%)		4.53			2.93			2.98			

Table 5
Computational results on the 100-node PRP instances.

Instance	DBL12				HEA++				
	NV	TD	TC	Time	NV	TD	TC	Dev	Time
UK100_01	14	2914.40	1240.79	1.54	14	2795.08	**1212.72***	−2.31	4.37
UK100_02	13	2690.40	1168.17	1.64	13	2660.65	**1149.16***	−1.65	4.67
UK100_03	13	2531.80	1092.73	3.47	13	2487.25	**1080.87***	−1.10	5.29
UK100_04	14	2438.50	1106.48	2.49	14	2374.23	**1085.66***	−1.92	5.13
UK100_05	14	2328.50	1043.41	2.65	14	2256.48	**1033.19***	−0.99	4.93
UK100_06	14	2782.40	1213.61	2.23	14	2733.05	**1192.67***	−1.76	4.83
UK100_07	12	2463.90	1060.08	1.71	12	2412.54	**1044.58***	−1.48	4.51
UK100_08	13	2597.40	1106.78	3.49	12	2524.80	**1092.67***	−1.29	5.67
UK100_09	13	2219.20	1015.46	2.57	13	2204.89	**992.36***	−2.33	4.97
UK100_10	12	2510.10	1076.56	3.32	12	2432.26	**1063.05***	−1.27	5.64
UK100_11	15	2792.10	1210.25	1.79	14	2722.22	**1200.53***	−0.81	4.11
UK100_12	12	2427.30	1053.02	3.44	12	2336.10	**1030.17***	−2.22	5.64
UK100_13	13	2693.10	1154.83	1.47	13	2589.17	**1132.02***	−2.01	3.49
UK100_14	14	2975.30	1264.50	1.53	14	2892.45	**1241.31***	−1.87	4.29
UK100_15	15	3072.10	1315.50	1.85	15	3038.40	**1311.36***	−0.32	3.87
UK100_16	12	2219.70	1005.03	4.25	12	2203.99	**986.57***	−1.87	5.97
UK100_17	15	2960.40	1284.81	2.55	15	2860.97	**1257.44***	−2.18	4.19
UK100_18	13	2525.20	1106.00	1.54	13	2506.71	**1088.89***	−1.57	4.21
UK100_19	13	2332.60	1044.71	1.52	13	2288.50	**1024.17***	−2.01	4.19
UK100_20	14	2957.80	1263.06	3.41	14	2915.17	**1249.84***	−1.06	5.17
Avg	13.4	2621.61	1141.29	2.42	13.3	2561.75	1123.46	−1.60	4.76
Min (%)								−2.33	
Max (%)								−0.32	
Processor	Xe 3.0 GHz				Xe 2.6 GHz				
Runs	10				10				

corresponding to an increase of 10.31%. It is clear that considering only distance in the objective results in a poor total cost performance, yielding a 4.11% increase. This increase is more substantial when looking only at the vehicle fixed cost where min TD is 8.65% higher in terms of VC. With respect to CO_2 emissions, the closest objective value is min TD + VC. This result implies that a substantial gain in CO_2 emissions can be achieved by using the TD + VC objective. However, minimizing CO_2 emissions yields an average increase of 1.09% in TC. Similar to the TD objective, the DC objective performs poorly on all cost components, yielding an average increase of 20.67% in the CO_2 emissions.

Table 6
Computational results on the 200-node PRP instances.

Instance	DBL12				HEA++				
	NV	TD	TC	Time	NV	TD	TC	Dev	Time
UK200_01	28	4609.60	2111.70	12.10	28	4545.77	**2067.00***	−2.16	14.20
UK200_02	24	4444.40	1988.64	17.00	25	4332.62	**1953.35***	−1.81	15.80
UK200_03	27	4439.90	2017.63	6.74	28	4365.82	**1996.13***	−1.08	10.40
UK200_04	26	4191.90	1934.13	6.86	26	4151.74	**1905.88***	−1.48	9.47
UK200_05	27	4861.90	2182.91	15.40	27	4848.28	**2151.99***	−1.44	16.80
UK200_06	27	3980.40	1883.22	7.51	27	3980.03	**1859.40***	−1.28	11.50
UK200_07	27	4415.30	2021.95	15.70	27	4276.06	**1974.32***	−2.41	17.90
UK200_08	27	4664.40	2116.76	7.17	27	4592.54	**2088.12***	−1.37	9.17
UK200_09	25	4031.10	1894.18	9.22	25	3932.44	**1823.50***	−3.88	11.70
UK200_10	28	4921.80	2199.95	8.33	27	4847.08	**2166.59***	−1.54	9.78
UK200_11	27	4099.50	1941.19	14.10	27	4126.44	**1908.83***	−1.70	16.30
UK200_12	25	4808.50	2105.14	11.90	26	4786.39	**2104.40***	−0.04	12.80
UK200_13	25	4760.30	2141.26	7.41	25	4734.21	**2094.48***	−2.23	9.37
UK200_14	27	4369.90	2011.35	7.51	27	4369.86	**1994.49***	−0.85	10.30
UK200_15	25	4723.90	2110.86	9.04	26	4642.58	**2067.48***	−2.10	11.40
UK200_16	27	4545.90	2075.83	7.59	27	4497.75	**2023.55***	−2.58	9.71
UK200_17	26	4972.80	2218.28	6.82	26	4915.18	**2165.34***	−2.44	8.97
UK200_18	27	4370.30	2004.68	13.20	27	4406.10	**2003.75***	−0.05	14.00
UK200_19	25	3995.40	1844.90	16.20	25	3946.49	**1803.56***	−2.29	17.50
UK200_20	27	4805.40	2150.57	8.85	26	4727.98	**2114.31***	−1.71	11.30
Avg	26.35	4500.60	2047.76	10.40	26.45	4451.27	2013.32	−1.72	12.40
Min (%)								−3.88	
Max (%)								−0.04	
Processor	Xe 3.0 GHz				Xe 2.6 GHz				
Runs	10				10				

Table 7
Average results on the FSMPRP instances.

Instance	TD	CO_2	FEC	DC	VC	TC	Time
75-node	1534.38	345.74	208.63	280.15	296.40	785.185	3.27
100-node	1841.48	414.17	249.93	354.56	375.00	979.484	4.79
150-node	2398.78	550.48	332.18	509.66	536.40	1378.24	7.03
200-node	2857.08	659.39	397.91	642.11	678.30	1720.42	10.4

Table 8
The effect of cost components: objective function values.

Objective	TD	CO_2	FEC	DC	VC	TC
Min TD (total distance)	1921.66	476.64	287.63	379.70	402	1069.31
Min FEC (fuel and emissions cost)	2119.87	371.10	223.91	444.40	370	1038.28
Min DC (driver cost)	2078.14	447.74	270.19	368.90	402	1041.13
Min TD and VC (total distance and vehicle fixed cost)	1994.23	407.14	245.69	410.40	384	1040.06
Min TC (total cost)	2031.46	444.12	268.00	375.10	384	1027.10

In order to quantify the added value of changing speeds, we have experimented with three other versions of the FSMPRP in which the speed on all arcs is fixed at 70, 85 or 100 km/h. Table 10 presents the results of these experiments. The results suggest that while optimizing speeds with HEA++ yields the best results, using a fixed speed of 100 km/h deteriorates the solution quality by only 1.16% on average. This makes sense since high driver costs will make it economical to drive fast. On the other hand, using a fixed speed of 70 km/h deteriorates the solution value by an average value of 15.19%.

5.4. The effect of the heterogeneous fleet

We now analyze the benefit of using a heterogeneous fleet of vehicles as opposed to using a homogenous fleet, coupled with using fixed versus variable speeds. To do so, we have conducted three sets of experiments on the 100-node FSMPRP instances, each corresponding to using a unique vehicle type, i.e., only light duty, only medium duty and only heavy duty vehicles. This results in three sets of PRP instances which are solved with the HEA++. We have compared these results with

Table 9
The effect of cost components: percent deviation from the minimum value

Objective	TD	CO_2	FEC	DC	VC	TC
Min TD (total distance)	0.00	28.46	28.46	2.91	8.65	4.11
Min FEC (fuel and emissions cost)	10.31	0.00	0.00	20.40	0.00	1.09
Min DC (driver cost)	8.14	20.67	20.67	0.00	8.65	1.37
Min TD and VC (total distance and vehicle fixed cost)	3.78	9.73	9.73	11.2	3.78	1.26
Min TC (total cost)	5.71	19.69	19.69	1.67	3.78	0.00

Table 10
The effect of the speed.

Instance	70 km/h		85 km/h		100 km/h		HEA++
	TC	Dev	TC	Dev	TC	Dev	TC
UK100_01	1218.01	18.01	1106.60	7.22	1032.10	0.49	1027.1
UK100_02	1154.54	13.31	1044.14	2.47	1018.94	1.60	1002.87
UK100_03	1066.70	13.88	982.49	4.89	936.69	1.80	920.11
UK100_04	1127.40	13.24	1028.27	3.28	995.57	0.33	992.31
UK100_05	1088.10	15.76	1007.40	7.18	939.93	0.90	931.56
UK100_06	1199.17	15.23	1099.62	5.66	1040.71	0.24	1038.25
UK100_07	1078.23	15.33	993.63	6.28	934.92	2.36	913.39
UK100_08	1128.36	14.26	1021.77	3.47	987.51	4.55	944.51
UK100_09	1059.50	17.76	963.49	7.09	899.68	0.97	891.02
UK100_10	1139.41	13.90	1055.82	5.55	1000.32	1.11	989.38
UK100_11	1197.71	14.92	1090.94	4.67	1042.25	0.70	1034.98
UK100_12	1023.51	16.19	942.27	6.97	880.87	0.10	879.96
UK100_13	1154.79	13.52	1054.11	3.63	1017.22	1.63	1000.86
UK100_14	1223.60	14.44	1112.03	4.01	1069.17	1.59	1052.47
UK100_15	1251.53	14.53	1156.86	5.86	1092.8	0.82	1083.95
UK100_16	1066.83	15.08	979.75	5.69	927.05	0.28	924.42
UK100_17	1254.68	17.99	1133.08	6.55	1063.41	0.58	1057.33
UK100_18	1091.80	15.77	991.94	5.18	943.05	2.19	922.81
UK100_19	1073.05	15.07	984.79	5.60	932.53	0.86	924.60
UK100_20	1223.29	15.56	1121.38	5.94	1058.54	0.07	1057.78
Average	1141.01	15.19	1043.52	5.36	990.66	1.16	979.48
Min (%)		13.24		2.47		0.07	
Max (%)		18.01		7.22		4.55	

Table 11
The effect of using a heterogeneous fleet.

Instance	Only light duty					Only medium duty					Only heavy duty				
	TC	Dev_{70}	Dev_{85}	Dev_{100}	Dev_V	TC	Dev_{70}	Dev_{85}	Dev_{100}	Dev_V	TC	Dev_{70}	Dev_{85}	Dev_{100}	Dev_V
UK100_01	1272.20	4.26	13.02	18.87	19.27	1066.34	−14.20	−3.78	3.21	3.68	1385.72	12.10	20.10	25.50	25.88
UK100_02	1236.88	6.67	15.58	17.62	18.92	1051.26	−9.82	0.68	3.07	4.60	1369.21	15.70	23.70	25.60	26.76
UK100_03	1208.80	11.76	18.72	22.51	23.88	928.30	−14.90	−5.84	−0.90	0.88	1209.97	11.80	18.80	22.60	23.96
UK100_04	1261.12	10.60	18.46	21.06	21.31	1013.97	−11.20	−1.41	1.81	2.14	1324.33	14.90	22.40	24.80	25.07
UK100_05	1242.92	12.46	18.95	24.38	25.05	1000.40	−8.77	−0.70	6.04	6.88	1304.31	16.60	22.80	27.90	28.58
UK100_06	1313.98	8.74	16.31	20.80	20.98	1058.53	−13.30	−3.88	1.68	1.92	1374.78	12.80	20.00	24.30	24.48
UK100_07	1130.95	4.66	12.14	17.33	19.24	930.84	−15.80	−6.75	−0.44	1.87	1204.82	10.50	17.50	22.40	24.19
UK100_08	1165.37	3.18	12.32	15.26	18.95	963.72	−17.10	−6.02	−2.47	1.99	1247.78	9.57	18.10	20.90	24.30
UK100_09	1121.13	5.49	14.06	19.75	20.52	918.53	−15.30	−4.90	2.05	2.99	1182.58	10.40	18.50	23.90	24.65
UK100_10	1137.93	−0.13	7.22	12.09	13.05	1034.73	−10.10	−2.04	3.33	4.38	1353.15	15.80	22.00	26.10	26.88
UK100_11	1305.80	8.28	16.45	20.18	20.74	1057.66	−13.20	−3.15	1.46	2.14	1376.04	13.00	20.70	24.30	24.79
UK100_12	1125.91	9.09	16.31	21.76	21.84	895.65	−14.30	−5.21	1.65	1.75	1170.16	12.50	19.50	24.70	24.80
UK100_13	1222.93	5.57	13.80	16.82	18.16	1042.52	−10.80	−1.11	2.43	4.00	1354.65	14.80	22.20	24.90	26.12
UK100_14	1323.30	7.53	15.97	19.20	20.47	1075.34	−13.80	−3.41	0.57	2.13	1400.69	12.60	20.60	23.70	24.86
UK100_15	1360.55	8.01	14.97	19.68	20.33	1087.52	−15.10	−6.38	−0.49	0.33	1417.90	11.70	18.40	22.90	23.55
UK100_16	1103.04	3.28	11.18	15.96	16.19	938.90	−13.60	−4.35	1.26	1.54	1202.76	11.30	18.50	22.90	23.14
UK100_17	1350.89	7.12	16.12	21.28	21.73	1078.64	−16.30	−5.05	1.41	1.98	1412.73	11.20	19.80	24.70	25.16
UK100_18	1141.93	4.39	13.13	17.42	19.19	939.68	−16.20	−5.56	−0.36	1.80	1216.87	10.30	18.50	22.50	24.17
UK100_19	1158.83	7.40	15.02	19.53	20.21	930.64	−15.30	−5.82	−0.20	0.65	1192.37	10.00	17.40	21.80	22.46
UK100_20	1283.81	4.71	12.65	17.55	17.61	1081.08	−13.20	−3.73	2.09	2.16	1396.63	12.40	19.70	24.20	24.26
Avg	1223.41	6.65	14.62	18.95	19.88	1004.71	−13.6	−3.92	1.36	2.49	1304.87	12.50	20.00	24.00	24.90
Min (%)		−0.13	7.22	12.09	13.05		−17.1	−6.75	−2.47	0.33		9.57	17.40	20.90	22.46
Max (%)		12.46	18.95	24.38	25.05		−8.77	0.68	6.04	6.88		16.60	23.70	27.90	28.58

Table 12
Capacity utilization rates.

Instance	Only light duty CU	Only medium duty CU	Only heavy duty CU	HEA++ CU
UK100_01	97.81	53.66	25.80	66.59
UK100_02	91.30	50.08	24.08	62.16
UK100_03	92.10	58.95	28.34	66.48
UK100_04	94.65	56.25	27.04	62.30
UK100_05	95.53	56.77	27.30	66.24
UK100_06	94.59	56.21	27.03	62.26
UK100_07	94.69	55.55	26.71	62.65
UK100_08	96.94	56.87	27.34	64.14
UK100_09	98.29	57.66	27.72	65.03
UK100_10	94.81	47.67	22.92	59.17
UK100_11	94.65	56.25	27.04	62.30
UK100_12	96.79	56.78	27.30	64.04
UK100_13	94.39	51.78	24.90	64.27
UK100_14	91.37	54.30	26.11	60.14
UK100_15	96.92	57.60	27.69	57.60
UK100_16	95.76	56.18	27.01	56.18
UK100_17	97.09	57.70	27.74	63.91
UK100_18	97.93	57.45	27.62	64.80
UK100_19	94.07	60.20	28.94	60.20
UK100_20	99.03	54.32	26.12	60.17
Avg	95.44	55.61	26.74	62.53
Min (%)	91.30	47.67	22.92	56.18
Max (%)	99.03	60.20	28.94	66.59

those of the four experiments shown in Table 10. Table 11 provides a summary of this comparison. The columns Dev_{70}, Dev_{85} and Dev_{100} respectively report the percentage increase in total cost as a result of using homogeneous vehicles as in Table 11 over the fixed-speed results shown in Table 10 for 70, 85 and 100 km/h. Similarly, the columns entitled Dev_V show the deviation in total cost between the various homogeneous cases and the FSMPRP, i.e., with HEA++. Table 11 suggests that the total cost increases when using a heavy duty homogeneous fleet. Compared to the FSMPRP this increase ranges from 22.46% to 28.58%. For the medium duty case, the total cost increase is on average 2.49% compared to the FSMPRP. With light duty vehicles, the average increase in total cost is 19.88% compared to the FSMPRP. These results imply that for the homogeneous case, it is preferable to use medium duty vehicles. It is clear that using a heterogeneous fleet of vehicles and optimizing their speeds is superior to using a homogeneous fleet of vehicles and optimizing their speeds. Table 11 also indicates that using a heterogeneous fleet of vehicles with a fixed speed of 100 km/h is better than using a homogeneous fleet of vehicles and optimizing their speeds with respect to the total cost. This implies that for our experimental setting heterogeneous fleet dimension is more important than speed optimization on each arc.

The final set of experiments we now present aim at providing some insight into the capacity utilization of the vehicle fleet, for both homogenous and heterogeneous cases. In Table 12, we present the capacity utilizations for the three PRP settings of Table 11 as well as for the FSMPRP. The column CU displays the percentage of capacity utilization for the vehicle fleet, which is calculated as 100 (total demand of route/ capacity of the vehicle). In contrast to the total cost, the capacity utilization reaches its maximum level (95.44%) and worse level (55.61%) when using only light duty or medium duty vehicles, respectively. Heavy duty vehicles have approximately six and two times more capacity than light duty and medium duty vehicles, respectively. The average capacity utilization for a heavy-duty only vehicle fleet is 26.74%, but this is probably due to the limitations imposed by the time window constraints. Using a heterogeneous fleet yields an average utilization of 62.53%, which is a compromise between light and heavy duty vehicles.

6. Conclusions

We have presented a hybrid evolutionary metaheuristic for the fleet size and mix pollution-routing problem (FSMPRP), which extends the pollution-routing problem (PRP) introduced by Bektaş and Laporte (2011) and further studied by Demir et al. (2012), to allow for the use of a heterogeneous vehicle fleet. The effectiveness of the algorithm was demonstrated through extensive computational experiments on realistic PRP and FSMPRP instances. These tests have enabled us to assess the effects of several algorithmic components and to measure the trade-offs between various cost indicators such as vehicle fixed cost, distance, fuel and emissions, driver cost and total cost. We have demonstrated the benefit of using a heterogeneous fleet over a homogeneous one. An interesting insight derived from this study is that using a heterogeneous fleet without speed optimization allows for a further reduction in total cost than using a homogeneous fleet with speed optimization. Furthermore, we have shown that using an adequate fixed speed yields results that are only slightly worse than optimizing the speed on each arc. This has a practical implication since it is easier to instruct drivers to hold a constant speed for their entire trip rather than change their speed on each segment.

Acknowledgments

The authors gratefully acknowledge funding provided by the Southampton Management School of University of Southampton and by the Canadian Natural Sciences and Engineering Research Council under grants 39682-10 and 436014-2013. Thanks are due to three referees for their valuable comments.

Appendix A

Tables A1–A4 present the detailed computational results on the 75, 100, 150, and 200-node FSMPRP instances. In all tables, columns TD, CO_2, FEC, DC, VC, TC and Time are as explained in the main body of text. Column Mix shows the resulting fleet composition where L, M and H refer to light, medium and heavy vehicles and the subscripts denote the number of such vehicles used in the fleet.

Table A.1
Computational results on the 75-node FSMPRP instances.

Instance	HEA++							
	TD	CO_2	FEC	DC	VC	Mix	TC	Time
UK75_01	1615.33	373.65	225.48	295.05	300	M^5	820.52	2.37
UK75_02	1295.66	289.32	174.59	268.08	282	L^1M^4	724.67	3.39
UK75_03	1565.67	349.94	211.17	274.58	282	L^1M^4	767.75	3.56
UK75_04	1322.99	298.26	179.99	274.17	282	L^1M^4	736.16	3.74
UK75_05	1559.89	358.89	216.57	274.98	300	M^5	791.56	3.27
UK75_06	1588.73	366.90	221.41	287.88	300	M^5	809.29	3.34
UK75_07	1586.55	367.38	221.70	294.25	300	M^5	815.94	2.81
UK75_08	1721.67	361.28	218.01	299.22	306	L^3M^3	823.23	3.35
UK75_09	1609.60	354.01	213.62	278.57	282	L^1M^4	774.19	3.49
UK75_10	1575.76	365.46	220.54	285.23	300	M^5	805.77	3.71
UK75_11	1161.03	255.72	154.31	247.39	282	L^1M^4	683.70	3.47
UK75_12	1445.46	334.10	201.61	260.38	300	M^5	761.99	3.19
UK75_13	1786.96	383.63	231.50	297.89	324	L^2M^4	853.39	2.59
UK75_14	1585.74	367.00	221.47	279.06	300	M^5	800.52	3.38
UK75_15	1707.01	366.13	220.94	296.41	324	L^2M^4	841.35	3.32
UK75_16	1536.76	356.44	215.09	277.45	300	M^5	792.54	3.93
UK75_17	1552.07	359.02	216.65	287.94	300	M^5	804.59	2.41
UK75_18	1483.53	327.60	197.69	274.30	282	L^1M^4	753.99	3.33
UK75_19	1467.55	328.35	198.14	269.84	282	L^1M^4	749.99	3.49
UK75_20	1519.60	351.64	212.20	280.38	300	M^5	792.57	3.19

Table A.2
Computational results on the 100-node FSMPRP instances.

Instance	HEA++							
	TD	CO_2	FEC	DC	VC	Mix	TC	Time
UK100_01	2031.46	444.12	268.00	375.10	384	L^2M^5	1027.10	5.47
UK100_02	1970.65	428.68	258.69	360.19	384	L^2M^5	1002.87	4.38
UK100_03	1756.29	392.38	236.78	341.34	342	L^1M^5	920.11	4.65
UK100_04	1674.29	384.01	231.73	358.58	402	L^1M^6	992.32	4.74
UK100_05	1583.76	368.75	222.52	349.04	360	M^6	931.56	4.21
UK100_06	1898.02	430.76	259.94	376.31	402	L^1M^6	1038.25	5.63
UK100_07	1790.55	400.89	241.91	329.48	342	L^1M^5	913.39	5.19
UK100_08	1919.84	424.64	256.25	346.27	342	L^1M^5	944.51	4.52
UK100_09	1633.23	364.06	219.69	329.33	342	L^1M^5	891.02	4.69
UK100_10	1955.77	429.26	259.04	346.34	384	L^2M^5	989.38	4.19
UK100_11	1904.88	429.65	259.27	373.71	402	L^1M^6	1034.98	5.13
UK100_12	1603.76	361.60	218.21	319.75	342	L^1M^5	879.96	4.62
UK100_13	1944.83	424.91	256.41	360.45	384	L^2M^5	1000.86	4.78
UK100_14	2025.79	454.55	274.30	376.17	402	L^1M^6	1052.47	5.02
UK100_15	1983.24	459.42	277.24	386.71	420	M^7	1083.95	5.27
UK100_16	1695.44	392.00	236.55	327.87	360	M^6	924.42	4.73
UK100_17	1980.20	447.53	270.06	385.27	402	L^1M^6	1057.33	4.36
UK100_18	1788.57	401.39	242.22	338.59	342	L^1M^5	922.81	5.01
UK100_19	1645.89	382.38	230.75	333.86	360	M^6	924.60	4.99
UK100_20	2043.21	462.36	279.01	376.77	402	L^1M^6	1057.78	4.18

Table A.3
Computational results on the 150-node FSMPRP instances.

Instance	HEA++							
	TD	CO_2	FEC	DC	VC	Mix	TC	Time
UK150_01	2142.69	486.39	293.51	490.91	522	L^1M^8	1306.42	6.28
UK150_02	2550.10	591.98	357.23	519.50	540	M^9	1416.73	6.78
UK150_03	2140.64	472.50	285.13	478.47	504	L^2M^7	1267.60	7.79
UK150_04	2385.71	555.33	335.11	520.18	540	M^9	1395.29	7.19
UK150_05	2284.05	521.09	314.45	493.46	522	L^1M^8	1329.91	6.47
UK150_06	2049.41	476.33	287.44	492.41	540	M^9	1319.85	7.13
UK150_07	2485.44	580.09	350.05	524.80	540	M^9	1414.86	7.34
UK150_08	2232.72	513.78	310.04	492.72	522	L^1M^8	1324.76	7.98
UK150_09	2587.83	581.73	351.04	529.16	564	L^2M^8	1444.20	6.37
UK150_10	2423.75	564.42	340.60	509.53	540	M^9	1390.13	6.93
UK150_11	2508.51	582.74	351.65	515.03	540	M^9	1406.69	7.96
UK150_12	2487.69	572.14	345.25	537.39	582	L^1M^9	1464.65	7.73
UK150_13	2437.12	556.33	335.72	506.81	522	L^1M^8	1364.52	6.67
UK150_14	2518.63	586.03	353.64	519.74	540	M^9	1413.38	6.67
UK150_15	2115.20	486.33	293.47	470.56	522	L^1M^8	1286.03	7.79
UK150_16	2515.94	570.23	344.11	517.33	522	L^1M^8	1383.43	7.07
UK150_17	2501.54	566.66	341.95	512.78	522	L^1M^8	1376.73	7.09
UK150_18	2389.19	554.28	334.48	502.72	540	M^9	1377.20	6.37
UK150_19	2509.16	584.23	352.55	523.01	540	M^9	1415.56	6.91
UK150_20	2710.19	606.91	366.24	536.72	564	L^2M^8	1466.96	6.09

Table A.4
Computational results on the 200-node FSMPRP instances.

Instance	HEA++							
	TD	CO_2	FEC	DC	VC	Mix	TC	Time
UK200_01	2844.46	649.17	391.74	664.28	702	L^1M^{11}	1758.02	9.48
UK200_02	2829.05	642.55	387.75	617.43	642	L^1M^{10}	1647.17	11.27
UK200_03	2780.80	649.79	392.12	650.58	660	M^{11}	1702.70	10.43
UK200_04	2694.43	628.51	379.27	629.06	660	M^{11}	1668.33	11.48
UK200_05	3018.01	691.92	417.54	661.99	702	L^1M^{11}	1781.53	10.12
UK200_06	2590.47	603.91	364.43	631.82	660	M^{11}	1698.24	9.79
UK200_07	2798.22	648.55	391.37	648.49	702	L^1M^{11}	1741.86	13.64
UK200_08	2888.09	660.78	398.75	660.65	702	L^1M^{11}	1761.40	8.64
UK200_09	2697.92	615.58	371.47	610.83	642	L^1M^{10}	1624.30	9.19
UK200_10	3036.77	696.08	420.05	668.45	702	L^1M^{11}	1790.50	11.28
UK200_11	2677.34	620.81	374.63	641.25	702	L^1M^{11}	1717.88	9.49
UK200_12	3147.88	731.72	441.56	642.67	660	M^{11}	1744.23	10.83
UK200_13	3052.43	712.56	430.00	639.22	660	M^{11}	1729.22	9.18
UK200_14	2845.53	648.49	391.33	648.09	702	L^1M^{11}	1741.42	9.49
UK200_15	2953.85	686.59	414.32	637.81	660	M^{11}	1712.13	11.28
UK200_16	2780.94	649.33	391.84	633.79	660	M^{11}	1685.63	9.79
UK200_17	3092.09	711.40	429.29	655.59	702	L^1M^{11}	1786.88	12.27
UK200_18	2832.24	656.36	396.08	645.11	702	L^1M^{11}	1743.19	9.79
UK200_19	2636.59	604.11	364.55	597.29	642	L^1M^{10}	1603.83	9.79
UK200_20	2944.54	679.61	410.11	657.80	702	L^1M^{11}	1769.91	11.35

References

Baldacci, R., Mingozzi, A., 2009. A unified exact method for solving different classes of vehicle routing problems. Mathematical Programming 120, 347–380.

Baldacci, R., Battarra, M., Vigo, D., 2008. Routing a heterogeneous fleet of vehicles. In: The Vehicle Routing Problem: Latest Advances and New Challenges. Springer, New York, pp. 1–25 (Chapter 1).

Barth, M., Boriboonsomsin, K., 2008. Real-world CO_2 impacts of traffic congestion. Tech. rep., Paper for the 87th Annual Meeting of Transportation Research Board. URL<http://www.uctc.net/papers/846.pdf> (accessed 21.01.2014).

Barth, M., Boriboonsomsin, K., 2009. Energy and emissions impacts of a freeway-based dynamic eco-driving system. Transportation Research Part D 14, 400–410.

Barth, M., Younglove, T., Scora, G. 2005. Development of a Heavy-duty Diesel Modal Emissions and Fuel Consumption Model. Technical Report. UCB-ITS-PRR-2005-1, California PATH Program, Institute of transportation Studies, University of California at Berkeley.

Bektaş, T., Laporte, G., 2011. The pollution-routing problem. Transportation Research Part B 45, 1232–1250.

Campbell, J.F., 1995a. Peak period large truck restrictions and a shift to off-peak operations: impact on truck emissions and performance. Journal of Business Logistics 16, 227–248.

Campbell, J.F., 1995b. Using small trucks to circumvent large truck restrictions: impacts on truck emissions and performance measures. Transportation Research Part A 29, 445–458.

Caterpillar, 2006. Tractor-trailer Performance Guide. Technical Report. URL<http://www.cat.com/cda/files/2222280/> (accessed 01.02.2014).
Clarke, G., Wright, J.W., 1964. Scheduling of vehicles from a central depot to a number of delivery points. Operations Research 12, 568–581.
Coe, E., 2005. Average Carbon Dioxide Emissions Resulting from Gasoline and Diesel Fuel, United States Environmental Protection Agency, Technical Report. URL<http://www.epa.gov/otaq/climate/420f05001.pdf> (accessed 11.02.2014).
Cordeau, J-F., Laporte, G., Mercier, A., 2001. A unified tabu search heuristic for vehicle routing problems with time windows. Journal of the Operational Research Society 52, 928–936.
DEFRA, 2007. Effects on Payload on the Fuel Consumption of Trucks. Technical Report. URL<http://www.freightbestpractice.org.uk/effects-of-payload-on-fuel-consumption-of-trucks> (accessed 15.02.2014).
DEFRA, 2012. Guidelines to DEFRA/ DECC GHG Conversion Factors for Company Reporting: Methodology Paper for Emission Factors. Technical Report. London, United Kingdom. URL <https://www.gov.uk/government/uploads/system/uploads/attachment_data/file/69568/pb13792-emission-factor-methodology-paper-120706.pdf> (accessed 17.02.2014).
Demir, E., Bektaş, T., Laporte, G., 2011. A comparative analysis of several vehicle emission models for road freight transportation. Transportation Research Part D 6, 347–357.
Demir, E., Bektaş, T., Laporte, G., 2012. An adaptive large neighborhood search heuristic for the pollution-routing problem. European Journal of Operational Research 223, 346–359.
Demir, E., Bektaş, T., Laporte, G., 2014a. The bi-objective pollution-routing problem. European Journal of Operational Research 232, 464–478.
Demir, E., Bektaş, T., Laporte, G., 2014b. A review of recent research on green road freight transportation. European Journal of Operational Research 237, 775–793.
DfT, 2010. Truck Specification for Best Operational Efficiency, United Kingdom Department for Transport, United Kingdom. URL: <http://www.freightbestpractice.org.uk/download.aspx?pid=124> (accessed 10.02.2014).
DfT, 2012. Reducing Greenhouse Gases and Other Emissions from Transport, United Kingdom Department for Transport, United Kingdom. URL: <http://www.gov.uk/government/policies/reducing-greenhouse-gases-and-other-emissions-from-transport> (accessed 15.02.2014).
EPA, 2012. DRAFT Inventory of United States Greenhouse Gas Emissions and Sinks: 1990–2012, United States Environmental Protection Agency, USA. URL: <http://www.epa.gov/climatechange/Downloads/ghgemissions/US-GHG-Inventory-2014-Main-Text.pdf> (accessed 15.02.2014).
FHWA, 2011. Vehicle Types, United States Department of Transport, FederaL Highway Administration, USA. URL: <http://www.fhwa.dot.gov/policy/ohpi/vehclass.htm> (accessed 25.02.2014).
Franceschetti, A., Honhon, D., Van Woensel, T., Bektaş, T., Laporte, G., 2013. The time-dependent pollution-routing problem. Transportation Research Part B 56, 265–293.
Golden, B.L., Assad, A.A., Levy, L., Gheysens, F., 1984. The fleet size and mix vehicle routing problem. Computers and Operations Research 11, 49–66.
Hoff, A., Andersson, H., Christiansen, M., Hasle, G., Løkketangen, A., 2010. Industrial aspects and literature survey: fleet composition and routing. Computers and Operations Research 37, 2041–2061.
Hvattum, L.M., Norstad, I., Fagerholt, K., Laporte, G., 2013. Analysis of an exact algorithm for the vessel speed optimization problem. Networks 62, 132–135.
Jabali, O., Van Woensel, T., de Kok, A.G., 2012. Analysis of travel times and CO_2 emissions in time-dependent vehicle routing. Production and Operations Management 21, 1060–1074.
Kirby, H.R., Hutton, B., McQuaid, R.W., Raeside, R., Zhang, X., 2000. Modelling the effects of transport policy levers on fuel efficiency and national fuel consumption. Transportation Research Part D 5, 265–282.
Koç, Ç., Bektaş, T., Jabali, O., Laporte, G., 2014. A Hybrid Evolutionary Algorithm for Heterogeneous Fleet Vehicle Routing Problems. Technical Report. CIRRELT 16, Montréal.
Kopfer, H.W., Kopfer, H., 2013. Emissions minimization vehicle routing problem in dependence of different vehicle classes. In: Kreowski, H-J., Reiter, B.S., Thoben, K-D. (Eds.), Dynamics in Logistics, Lecture Notes in Logistics. Springer, Berlin, pp. 49–58.
Kopfer, H.W., Schönberger, J., Kopfer, H., 2014. Reducing greenhouse gas emissions of a heterogeneous vehicle fleet. Flexible Services and Manufacturing Journal 26, 221–248.
Kwon, Y.J., Choi, Y.J., Lee, D.H., 2013. Heterogeneous fixed fleet vehicle routing considering carbon emission. Transportation Research Part D 23, 81–89.
MAN, 2014a. Trucks in Distribution Transport. URL: <http://www.mantruckandbus.co.uk/en/trucks/start_trucks.html> (accessed 26.02.2014).
MAN Engines, 2014b. URL: <http://www.engines.man.eu/global/en/index.html#7906576> (accessed 05.08.2014).
MAN Spec Sheets, 2014c. URL: <http://www.man-bodybuilder.co.uk/specs/euro6/> (accessed 05.08.2014).
Mercedes-Benz, 2014. Distribution. URL: <http://www2.mercedes-benz.co.uk/content/unitedkingdom/mpc/mpc_unitedkingdom_website/en/home_mpc/truck/home/new_trucks/showroom.flash.html> (accessed 24.03.2014).
Nagata, Y., Bräysy, O., Dullaert, W., 2010. A penalty-based edge assembly memetic algorithm for the vehicle routing problem with time windows. Computers and Operations Research 37, 724–737.
Norstad, I., Fagerholt, K., Laporte, G., 2010. Tramp ship routing and scheduling with speed optimization. Transportation Research Part C 19, 853–865.
Paraskevopoulos, D.C., Repoussis, P.P., Tarantilis, C.D., Ioannou, G., Prastacos, G.P., 2008. A reactive variable neighbourhood tabu search for the heterogeneous fleet vehicle routing problem with time windows. Journal of Heuristics 14, 425–455.
Pisinger, D., Ropke, S., 2007. A general heuristic for vehicle routing problems. Computers and Operations Research 34, 2403–2435.
Prins, C., 2009. Two memetic algorithms for heterogeneous fleet vehicle routing problems. Engineering Applications of Artificial Intelligence 22, 916–928.
Renault, 2014. Distribution. URL: <http://www.renault-trucks.co.uk/> (accessed 21.02.2014).
Ribeiro, S.K., Kobayashi, S., Beuthe, M., Gasca, J., Greene, D., Lee, D.S., Muromachi, Y., Newton, P.J., Plotkin, S., Sperling, D., Wit, R., Zhou, P.J., 2007. Transport and its infrastructure. In: Climate Change 2007: Mitigation. URL: <http://www.ipcc.ch/pdf/assessment-report/ar4/wg3/ar4-wg3-chapter5.pdf> (accessed 27.02.2014).
Ropke, S., Pisinger, D., 2006a. An adaptive large neighborhood search heuristic for the pickup and delivery problem with time windows. Transportation Science 40, 455–472.
Ropke, S., Pisinger, D., 2006b. A unified heuristic for a large class of vehicle routing problems with backhauls. European Journal of Operational Research 171, 750–775.
Scora, M., Barth, G., 2006. Comprehensive Modal Emission Model (CMEM), Version 3.01, User Guide. Technical Report. URL: <http://www.cert.ucr.edu/cmem/docs/CMEM_User_Guide_v3.01d.pdf> (accessed 17.02.2014).
Statista, 2013. Market Share of Truck Manufacturers in Europe. URL: <http://www.statista.com/statistics/265008/market-share-of-truck-manufacturers-in-europe/> (accessed 29.07.2014).
Taillard, ÉD., 1999. A heuristic column generation method for the heterogeneous fleet vehicle routing problem. RAIRO (Recherche Opérationnelle/Operations Research) 33, 1–14.
Vidal, T., Crainic, T.G., Gendreau, M., Prins, C., 2014. A unified solution framework for multi-attribute vehicle routing problems. European Journal of Operational Research 234, 658–673.
Volvo, 2014. City and Urban Transports. URL: <http://www.volvotrucks.com/trucks/uk-market/en-gb/trucks/Pages/trucks.aspx> (accessed 22.02.2014).